Title
Engineered polymer nanoparticles incorporating l-amino acid groups as affinity reagents for fibrinogen

Journal
Journal of Pharmaceutical Analysis, 11(5)

ISSN
2095-1779

Authors
Zhu, Yongyan
Liu, Ruixuan
Wu, Dengyu
et al.

Publication Date
2021-10-01

DOI
10.1016/j.jpha.2020.10.004

Peer reviewed

Journal of Pharmaceutical Analysis 11 (2021) 596–602

Contents lists available at ScienceDirect

Journal of Pharmaceutical Analysis

journal homepage: www.elsevier.com/locate/jpa

Original article

Engineered polymer nanoparticles incorporating L-amino acid groups as affinity reagents for fibrinogen

Yongyan Zhu [a, b, c, 1], Ruixuan Liu [a, 1], Dengyu Wu [a], Qianqian Yu [a], Kenneth J. Shea [d, **], Quanhong Zhu [a, b, c, *]

[a] School of Traditional Chinese Medicine, Southern Medical University, Guangzhou, 510515, China
[b] Guangdong Provincial Key Laboratory of Chinese Medicine Pharmaceutics, Guangzhou, 510515, China
[c] Guangdong Provincial Engineering Laboratory of Chinese Medicine Preparation Technology, Guangzhou, 510515, China
[d] Department of Chemistry, University of California, Irvine, CA, 92697, USA

ARTICLE INFO

Article history:
Received 21 January 2020
Received in revised form
17 October 2020
Accepted 19 October 2020
Available online 22 October 2020

Keywords:
Synthetic polymer nanoparticles
Amino-acid monomers
Arginine
Fibrinogen
Affinity reagent
Protein interaction

ABSTRACT

Synthetic polymer hydrogel nanoparticles (NPs) were developed to function as abiotic affinity reagents for fibrinogen. These NPs were made using both temperature-sensitive N-isopropyl acrylamide (NIPAm) and L-amino acid monomers. Five kinds of L-amino acids were acryloylated to obtain functional monomers: L-phenylalanine (Phe) and L-leucine (Leu) with hydrophobic side chains, L-glutamic acid (Glu) with negative charges, and L-lysine (Lys) and L-arginine (Arg) with positive charges. After incubating the NPs with fibrinogen, γ-globulin, and human serum albumin (HSA) respectively, the NPs that incorporated N-acryloyl-Arg monomers (AArg@NPs) showed the strongest and most specific binding affinity to fibrinogen, when compared with γ-globulin and HSA. Additionally, the fibrinogen-AArg binding model had the best docking scores, and this may be due to the interaction of positively charged AArg@NPs and the negatively charged fibrinogen D domain and the hydrophobic interaction between them. The specific adsorption of AArg@NPs to fibrinogen was also confirmed by the immunoprecipitation assay, as the AArg@NPs selectively trapped the fibrinogen from a human plasma protein mixture. AArg@NPs had a strong selectivity for, and specificity to, fibrinogen and may be developed as a potential human fibrinogen-specific affinity reagent.

1. Introduction

Fibrinogen, a primary component of human plasma protein, plays a vital role in the process of blood coagulation [1] and usually circulates at a concentration of between 2 and 4 g/L in the human body [2]. Fibrinogen treatments for patients with massive bleeding are essential for survival [3], and the amount of fibrinogen administered to trauma patients is positively correlated with reductions in mortality [4]. The various sources of fibrinogen for replenishment include fresh frozen plasma, cryoprecipitate, and fibrinogen concentrate [5]. The former two are allogeneic blood products and have numerous safety concerns [5,6], while fibrinogen concentrate has a better safety profile, making it a preferred method for fibrinogen supplementation [6]. The advantages of fibrinogen concentrate include rapid administration of a standardized dose of fibrinogen, the lack of a need for blood type screening, and being virally inactive and storing the product at room temperature (2–25 °C) [6]. Fibrinogen concentrate is commercially available as a pasteurized, lyophilized powder, and is mainly manufactured from human plasma by cryoprecipitation. However, the precipitate obtained from the cryoprecipitation process lacks selectivity and specificity, and the purification process (currently in use) is complex, as it requires a series of viral inactivation and removal process steps [6]. Therefore, the aim of this study is to engineer a novel polymeric nanoparticle that can act as a protein affinity reagent for human fibrinogen that can selectively capture fibrinogen from human plasma, thus developing a new way to manufacture fibrinogen concentrate.

Synthetic polymer nanoparticles (NPs) that can selectively

Peer review under responsibility of Xi'an Jiaotong University.
* Corresponding author. School of Traditional Chinese Medicine, Southern Medical University, Guangzhou, 510515, China.
** Corresponding author.
E-mail addresses: kjshea@uci.edu (K.J. Shea), zqh@smu.edu.cn (Q. Zhu).
[1] These authors contributed equally to this work.

https://doi.org/10.1016/j.jpha.2020.10.004

capture target proteins in biological fluids are a novel class of materials that have gained much attention for their role in protein recognition and separation [7]. Vijayan et al. [8] prepared polylactic acid-glycolic acid nanoparticles (PLGA-NPs) that encapsulated vascular endothelial growth factor (VEGF) and basic fibroblast growth factor (bFGF) which were conjugated to an antimicrobial peptide (K4). The resulting NP-protein complex had a high encapsulation rate, demonstrated a sustained release behavior, and enhanced angiogenesis. Shea's research group have also shown the effect of NP composition on the affinity to target proteins. They demonstrated the selective capture and programmed release of lysozyme from complex protein mixtures (egg white) [9], specificity to the Fc domain of IgG [7], in vitro and in vivo inhibit binding of vascular endothelial growth factor (VEGF165) to its receptor [10] and the sequestration/neutralization of the peptide toxin melittin [11] or the venomous protein phospholipase A2 [12].

Natural amino acids are the basic units of proteins, and the various recognitions, i.e., protein-protein, ligand-receptor, and antigen-antibody, depend on the amino acid side chains present. In recent years, natural amino acids have been shown to be the preferential building units for synthetic polymer nanoparticles [13], and the amino acid-based polymers have been widely evaluated in a variety of fields. These include chiral recognition [13], artificial abiotic inhibitors [14], and delivery systems for small molecule drugs [15,16], or proteins [17]. This is because of their chiral chemical structure [13], polyelectrolyte character [18], facile chemical modification [19], potential nontoxicity, and biocompatibility [14,16]. On account of a variety of functional pendant groups of amino acid monomers, a synthetic polymer hydrogel could be easily formulated with amino acid functional groups complementary to protein domains or peptide targets. Like natural protein, amino acid side chains of polymers could interact with target protein via strong non-covalent interactions, such as hydrogen bonds, ionic bonds, electrostatic interactions, hydrophobic effects, and van der Waals force [20].

Based on the structures and properties of polymers composed of amino acids, we introduced acryloyl groups into L-amino acids with different side chains to gain five different amino acid monomers. Then we engineered five N-isopropylacrylamide (NIPAm) based polymer NPs using these amino acids as co-monomers in aqueous solution by free radical polymerization. The affinity of these NPs to human plasma protein (human serum albumin (HSA), fibrinogen, and γ-globulin) was evaluated to find the optimal composition of NPs that could selectively capture fibrinogen from the human plasma protein complex, and aid in the development of an affinity reagent for fibrinogen.

2. Materials and methods

2.1. Materials

L-phenylalanine, L-leucine, L-glutamic acid, L-lysine, L-arginine, acryloyl chloride, N-isopropylacrylamide (NIPAm), hexadecyltrimethylammonium bromide (CTAB), ammonium persulfate (APS), sodium dodecyl sulfate (SDS), N,N′-methylenebisacrylamide (BIS), and N-t-butylacrylamide (TBAm) were purchased from TCI Development Co., Ltd. (Shanghai, China). Azobisisobutyronitrile (AIBN) was obtained from Fuchen Chemical Reagent Factory (Tianjin, China) and recrystallized with methanol. Tetramethylethylenediamine (TEMED), fibrinogen, γ-globulin, and human serum albumin (HSA) were purchased from Sigma-Aldrich Co., LLC. (Shanghai, China). Protein ladder was purchased from Thermo Fisher Scientific Co., Ltd. (Shanghai, China).

2.2. Synthesis of amino acid monomers

The monomers N-acryloyl-L-phenylalanine (APhe) [21], N-acryloyl-L-leucine (ALeu) [22], N-acryloyl-L-glutamic acid (AGlu) [23], N-acryloyl-L-lysine (ALys) [17] and N-acryloyl-L-arginine (AArg) [24] were synthesized according to the referenced methods, and the yields were 45.7%, 74.30%, 37.75%, 62.20%, and 66.24%, respectively. ^{1}H NMR spectroscopy (400 MHz; Varian, Palo Alto, CA, USA) was used to evaluate the structures of products (Figs. S1–S5).

APhe: ^{1}H NMR (400 MHz, MeOD) δ (ppm) 7.16–7.27 (m, 5H, Ar–*H*), 6.18–6.28 (m, 2H, C*H*H=*CH*CO-), 5.62 (d, 1H, CH*H*=CHCO-), 4.71–4.75 (m, 1H, –HN–C*H*(CH_2-)COOH), 3.22 (d, 1H, Ar-C*H*H-(HN)CHCOOH), 2.98 (d, 1H, Ar-CH*H*-(HN)CHCOOH).

ALeu: ^{1}H NMR (400 MHz, $CDCl_3$) δ (ppm) 7.26 (brs, 1H, NH), 6.72 (d, 1H, CHH=C*H*-), 5.93–5.86 (dd, 1H, C*H*H=CH-), 5.37 (d, 1H, CH*H*=CH-), 4.38–4.33 (m, 1H, NHC*H*(CH_2-)COOH), 1.43–1.37 (m, 2H, CH_2CH(CH_3)$_2$), 1.37–1.30 (m, 1H, CH_2CH(CH_3)$_2$), 0.63 (dd, 6H, CH_2CH(CH_3)$_2$).

AGlu: ^{1}H NMR (600 MHz, CD_3OD) δ (ppm) 6.30 (d, 1H, CHH=*CH*CO-), 6.20 (d, 1H, C*H*H=CHCO-), 5.70 (m, 1H, CH*H*=CHCO-), 4.51 (dd, 1H, NHC*H*(CH_2-)COOH), 2.2 (m, 2H, NH–CH_2–CH_2-), 2.0 (m, 2H, NH–CH_2–CH_2–CH_2-)

ALys: ^{1}H NMR (400 MHz, CD_3OD) δ (ppm) 6.33–6.27 (m, 1H, CHH=*CH*CO-), 6.20 (dd, 1H, C*H*H=*CH*CO-), 5.66–5.62 (m, 1H, CH*H*=CHCO-), 4.40 (dt, 1H, –HN–C*H*(CH_2-)COOH), 2.98 (dt, 2H, NH_2–CH_2–CH_2–CH_2–CH_2-), 1.89–1.66 (m, 2H, NH_2–CH_2–CH_2–CH_2–CH_2-), 1.50–1.43 (m, 2H, NH_2–CH_2–CH_2–CH_2–CH_2-), 1.26–1.13 (m, 2H, NH_2–CH_2–CH_2–CH_2–CH_2-).

AArg: ^{1}H NMR (400 MHz, CD_3OD) δ(ppm) 6.23–6.17 (dd, 1H, C*H*=CH_2), 6.04 (d, 1H, J = 16 Hz, CH=C$H_{2\ trans}$), 5.49 (m, 1H, J = 12 Hz, CH=C$H_{2\ cis}$), 4.22 (s, 1H, –HN–C*H*(CH_2-) COOH), 3.05–3.00 (m, 2H, CH_2–CH_2–CH_2–CH–HN), 1.77–1.56 (m, 2H, CH_2–CH_2–CH_2–CH–HN), 1.48–1.59 (m, 2H, CH_2–CH_2–CH_2–CH–HN).

2.3. Preparation and characteristics of NPs

2.3.1. Preparation of NPs with hydrophobic amino acid monomers

NPs with hydrophobic amino acid side chains (APhe@NPs and ALeu@NPs) were synthesized using previously reported procedures [12] with a few modifications. NIPAm (93% (mol/mol)) and hydrophobic amino acid monomers (APhe, ALeu; 5% (mol/mol)) were dissolved in water (50 mL) with BIS (2% (mol/mol)) and SDS (30 mg, 1 μmol); the final monomer concentration was 65 mM. Ammonium persulfate (30 mg dissolved in 1 mL H_2O) was added, and the resulting solution was degassed with nitrogen for 30 min while stirring. The reaction was performed at 60 °C under a nitrogen atmosphere for 3 h to allow for polymerization, after which the mixture was quenched by exposure to air. The reaction mixture was then transferred to dialysis bag (molecular weight cutoff 12,000–14,000; Fisher Scientific, Pittsburgh, PA, USA) and dialyzed against double deionized water (changed twice a day) for 4 days. After dialysis, 5 mL of the NP solution was lyophilized to determine the weight-based concentration and yield.

2.3.2. Preparation of NPs with positive and negative charges

Positively charged NPs (ALys@NPs and AArg@NPs) were synthesized according to the reported procedures [25] with some modifications. NIPAm (53% (mol/mol)), positively charged monomer (ALys or AArg; 5% (mol/mol)), TBAm (40% (mol/mol)), BIS (2% (mol/mol)) and CTAB (20 mg) were dissolved in water (50 mL). TBAm was dissolved in 1 mL of ethanol before addition to the monomer solution, resulting in a total monomer concentration of 65 mM. The resulting solutions were degassed with nitrogen for 30 min. Following the addition of AIBN acetone solution (30 mg/

Table 1
The composition of NPs [a].

NPs	Feed ratio of functional monomers (%)							Yield (%)	Incorporation ratio of NIPAm to amino acid monomers
	NIPAm	TBAm	APhe	ALeu	AGlu	ALys	AArg		
APhe@NPs	93	0	5	0	0	0	0	85.72	93:4.6
ALeu@NPs	93	0	0	5	0	0	0	87.63	91.9:5
AGlu@NPs	53	40	0	0	5	0	0	89.90	53:4.8
ALys@NPs	53	40	0	0	0	5	0	84.12	53:4.5
AArg@NPs	53	40	0	0	0	0	5	78.40	49:5

[a] All NPs contain 2% (mol/mol) BIS with the indicated amounts of functional monomer.

500 μL), the polymerization reaction was carried out at 60–65 °C for 3 h under a nitrogen atmosphere. The polymerized solution was purified by dialysis against double distilled water (changed twice a day) for 4 days, after which 5 mL of the NP solution was lyophilized to determine the weight-based concentration and yield.

A similar procedure was used to prepare the negatively charged NPs (AGlu@NPs). Specifically, a negatively charged monomer was used, combined with APS substituted for AIBN (initiator) and SDS substituted for CTAB (surfactant).

2.3.3. Characteristics of the engineered NPs

The structures of these polymers were evaluated by ^{1}H NMR using a Fourier transform superconducting magnetic resonance spectrometer (AVANCE III™ HD 600 MHz; Bruker Biospin, Rheinstetten, Germany). The average hydrodynamic diameter and polydispersity index (PDI) of the polymers were determined by dynamic light scattering (DLS; Nano S90, Malvern, UK).

2.4. Binding of NPs to proteins

NP interactions with three human plasma proteins, including fibrinogen, γ-globulin, and HSA, were evaluated by UV–visible spectrometry (HP8453; Agilent, Carpinteria, CA, USA). Protein was dissolved in phosphate-buffered saline (PBS; pH 7.4, 10 mmol/L) and mixed with an NP (APhe@NPs, ALeu@NPs, AGlu@NPs, ALys@NPs, or AArg@NPs) solution to give a total volume of 1 mL (final concentrations of proteins and NPs were 2 mg/mL and 1 mg/mL, respectively). The NP-protein solution was incubated at 37 °C for 30 min. Samples were centrifuged at 14,500 rpm for 15 min, and the supernatant was filtered through a 0.22 μm syringe filter to remove the NPs and protein-bound NPs. Interactions between the protein and NPs were indirectly evaluated by measuring the absorbance of the supernatant and the initial protein solution at 280 nm. The binding amount (%) of the protein to NPs was calculated using Equation (1) [25].

$$\textit{Binding rate}\ (\%) = \left[1 - \left(A_{\text{supernatant}}/A_{\text{protein}}\right)\right] \times 100\% \qquad (1)$$

2.5. Molecular docking study to assess the interaction forces between fibrinogen and amino acid monomers

Five amino acid monomers, including APhe, ALeu, AGlu, ALys, and AArg, were tested in the molecular docking study with human fibrinogen fragment D using DOCK 6 [26]. Firstly, constructions of five amino acid monomers served as the ligands were drawn and optimized via chimera 1.6.1 with three-dimensional orientation (connection errors were checked). Hydrogen atoms were added (pH 7.2), and charges were also added using the Merck Molecular Force Field 94 (MMFF94) method, and then energy was minimized using the MMFF94s force field with the maximum step of 1000. The crystal structure of human fibrinogen fragment D (PDB ID: 1FZA) was retrieved from the Protein Data Bank (http://www.rcsb.org/) and used as a receptor of the experimental object. For the preparation of the molecular docking, all water molecules of the protein's crystal structure were removed, and hydrogen atoms were added. The co-crystalline ligand was N-acetyl-D-glucosamine, of which the binding position would be the docking pocket. Then molecular docking was performed using a flexible docking model. Other parameters were set to default.

2.6. Selective binding of AArg@NPs to fibrinogen

Selective binding of AArg@NPs with fibrinogen was analyzed by sodium dodecyl sulfate-polyacrylamide gel electrophoresis (SDS-PAGE). Solution of protein mixtures (fibrinogen, γ-globulin, and HSA) was prepared in PBS buffer (10 mmol/L, pH 7.4) and mixed with solution containing AArg@NPs to give a final volume of 1 mL (final concentrations of proteins and AArg@NPs were 500 μg/mL and 1 mg/mL, respectively). The NP-protein solution was incubated at 37 °C for 30 min. Samples were centrifuged at 14,500 rpm for 15 min, and the supernatant was filtered through a 0.22 μm syringe filter and collected for SDS-PAGE analysis. Subsequently, the centrifugal precipitate was re-suspended in 200 μL of PBS at room temperature, and then washed and centrifuged twice. The pellet was mixed with 200 μL of PBS and oscillated at 4 °C for 30 min to elute the protein that bound to the AArg@NPs. The solution was centrifuged at 14,500 rpm for 15 min, and the supernatant was filtered through a 0.22 μm syringe filter for SDS-PAGE analysis. The resulting protein samples for SDS-PAGE analysis were treated with lysis solution and then heated at 100 °C for 3 min. After running the samples, the SDS-PAGE gel (12% precast gel) was stained with Coomassie Brilliant Blue G250.

3. Results and discussion

3.1. Preparation and characteristics of NPs with amino acid residues

Amino acid-based polymers with chiral structures and a variety of side groups are the preferred candidates for affinity purification of homochiral biological polymers such as proteins, RNA, and DNA. Hence, five natural amino acids with different side chains, including two hydrophobic, one negatively charged and two positively charged, were acryloylated to produce the corresponding amino acid monomers, namely, APhe, ALeu, AGlu, ALys and AArg. A small library of hydrogel NPs were synthesized by precipitation polymerization NIPAm as the core monomer combined with various kinds of amino acid monomers (Table 1). The hydrophobic monomer, TBAm (40% (mol/mol)) was incorporated into the negatively charged polymers (AGlu@NPs) and positively charged polymers (ALys@NPs and AArg@NPs) to synthesize homologous NPs [27], and to enhance their hydrophobicity to stabilize the NP binding to proteins [25]. BIS (2% (mol/mol) of total monomer composition) was incorporated as a cross-linker. The slightly cross-linked polymers allowed the side chains of polymers to more

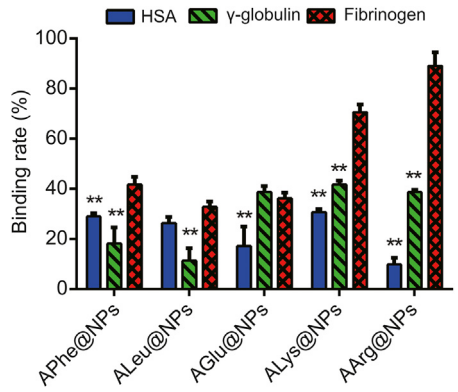

Fig. 1. Interaction of NPs carrying amino acid pendants with various proteins evaluated by UV–visible spectrometry. The binding amount ratio of the protein to the NPs was calculated by the absorbance at 280 nm. (Values are expressed as mean ± SD, n=3. $^{**}P < 0.05$ compared with fibrinogen groups.)

flexibly and firmly "map" onto a protein surface with complementary functional groups [7].

DLS experiments were carried out to assess the PDI, physical stability, and average hydrodynamic diameter of NPs. All NPs were monomodal and behaved as stable colloidal suspensions in water at a nano-scale size (average diameter less than 200 nm). The incorporation ratio of amino acid monomers to NIPAm were analyzed by ^{1}H NMR (Table 1). The signal at 4.0–4.7 ppm corresponded to the methine proton that linked with carboxyl and amine groups of amino acid monomers in NPs. The peak at 3.5–4.0 ppm was ascribed to the methine proton connected with the isopropyl group of NIPAm [28] (Figs. S6–S10). The results confirmed that the amino acid residues were incorporated into the NIPAm based nanohydrogels.

Since NIPAm has minimal innate biomacromolecule affinity, we used the NIPAm as the base monomer for the synthesis of these five NPs. From this, we showed direct correlations between the addition of functional monomers and the affinity of NPs to the target proteins [29]. Furthermore, the NPs, combined with NIPAm, were temperature-responsive. Below their lowest critical solution temperature (LCST), NPs were swollen, highly hydrated, and hydrophilic, while above their LCST, they were collapsed and more hydrophobic as a result of an entropically driven dissociation of water molecules [9].

When a balanced amount of amino acid monomers was incorporated, the NPs (APhe@NPs, ALeu@NPs, and AGlu@NPs) all underwent a volume-phase transition from a solvent swollen "hydrophilic" state to the collapsed "hydrophobic" state with the increase of temperature. The LCST of the APhe@NPs, ALeu@NPs, and AGlu@NPs was 32, 29, and 14 °C, respectively, in water (Figs. S11–S13). However, two NPs carrying the positively charged side chains showed the opposite temperature-responsive behavior. As the temperature increased, the size of ALys@NPs and AArg@NPs both started to increase quickly at their corresponding critical phase transition temperature, 12 °C and 16 °C, respectively, which suggested that AArg@NPs would become aggregated above 16 °C but dispersed below 16 °C (Fig. S14 and Fig. S15).

3.2. The effect of NP composition on the affinity of NPs to proteins

The binding ability of NPs to human plasma proteins was evaluated by co-incubating NPs (2 mg/mL) and three proteins (HSA, γ-globulin, or fibrinogen at 1 mg/mL) in PBS. After centrifugation, the concentration of free protein in the supernatant was estimated by UV–visible spectrometry. The results of binding experiments are summarized in Fig. 1.

The binding rates of NPs to HSA, γ-globulin, and fibrinogen were not more than 50% when incorporated into hydrophobic (APhe and ALeu) and negatively charged (AGlu) amino acid monomers (Fig. 1). However, there were significant differences in the binding rates of these two kinds of NPs to the three test proteins. Interestingly, AArg@NPs and ALys@NPs, composed of amino acids with positively charged side chains, were observed to have strong binding to fibrinogen, and the binding rates were 89.14% ± 5.31% and 70.61% ± 3.02%, respectively. In contrast, the AArg@NPs and ALys@NPs exhibited low binding rates to HSA and γ-globulin. Therefore, this indicated that the NPs with positively charged amino acids demonstrated a significant affinity to fibrinogen.

Fibrinogen, whose isoelectric point (pI) is 5.5, is relatively hydrophobic and negatively charged at physiological pH. The fibrinogen consists of six chains (two Aα, two Bβ, and two γ chains) arranged in an elongated manner (45 nm). The N-termini are located in a central nodule called the E domain, while the C-termini of Bβ and two γ chains form the two outer globular folds called the D domains, forming a "dumbbell-shaped" structure (Fig. 2A). The E domain is capped with two sets of negatively charged fibrinopeptides, A and B, which can be cleaved by thrombin to expose the positively charged E_A and E_B, respectively (Fig. 2B). This then initiates the end-to-middle intermolecular associations between the positively charged E_A and E_B surfaces and the negatively charged D domain, resulting in homocomplex fibril assembly [25,28–32]. Therefore, we sought to synthesize one abiotic NP to mimic the positively charged E_A and E_B, which would be complementary to the hydrophobic and negatively charged D domain.

Since AArg and TBAm were prepared as co-monomers, we inferred that AArg@NPs carried a positive charge and had a hydrophobic domain. Because of affinity to the E_A and E_B surfaces, AArg@NPs presented a protein-like interface to the negatively charged and hydrophobic D domain of fibrinogen via the coordination forces regulated by electrostatic and hydrophobic interactions. As for ALys@NPs, the ionization ability of the primary amine on ALys@NPs was weaker than that of guanidine groups on AArg@NPs. Thus, it displayed weaker electrostatic interactions with fibrinogen, which may be one of the main reasons for the lower binding capacity observed when compared with AArg@NPs. Additionally, the weaker hydrogen bond of ALys@NPs to fibrinogen may contribute to the lower binding capacity compared with AArg@NPs. Here, the guanidine groups on AArg@NPs could form two hydrogen bonds with fibrinogen, but only one hydrogen bond between the primary amine group of ALys@NPs and fibrinogen [25]. Therefore, it was reasonable to observe minimal binding of APhe@NPs, ALeu@NPs, and AGlu@NPs to fibrinogen as a result of weaker hydrophobic interactions and charge repulsion.

HSA also possesses negatively charged outer surfaces (pI=4.6) and hydrophobic pockets, similar to fibrinogen. However, the binding amount of AArg@NPs (9.92% ± 2.63%) and ALys@NPs (30.69% ± 1.37%) to HSA was decreased compared with fibrinogen (AArg@NPs: 89.14% ± 5.31%; ALys@NPs: 70.61% ± 3.02%) (P<0.01). This may be attributed to the different hydrophobic pockets of HSA compared with fibrinogen, which is buried inside the protein and just available to small-molecule ligands [25]. This means that hydrophobic pockets of HSA were inaccessible to NPs, and this resulted in weaker interactions between NPs and HSA. With respect to the neutral γ-globulin (pI=6.9), the binding rates of the positively charged AArg@NPs and ALys@NPs were 38.70% ± 1.02% and 41.71% ± 1.64%, much lower than that between AArg@NPs and fibrinogen (P<0.01) or between ALys@NPs and fibrinogen (P<0.01), respectively, and this was probably because of the lack of electrostatic interactions with γ-globulin. The results above indicate that the positively charged AArg@NPs and ALys@NPs displayed specific

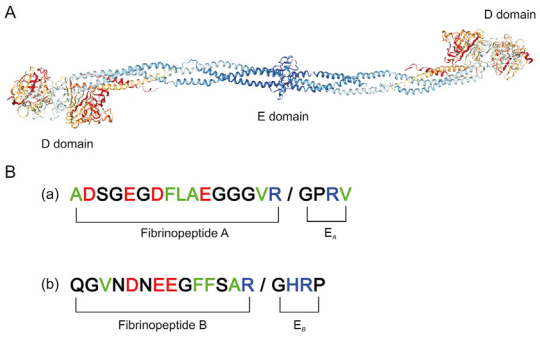

Fig. 2. (A) The X-ray crystal structure of fibrinogen (PDB ID: 3GHG), and (B) sequences of fibrinopeptide and N-terminals of fibrin polymerization sites in the E domain reported by the Shea research group [25]. (a) Fibrinopeptide A and N-terminal of E_A site on fibrinogen Aα-chain (UniProt: P02671), and (b) fibrinopeptide B and N-terminal of E_B site on fibrinogen Bβ-chain (UniProt: P02675). Red, blue and green fonts indicate negatively charged, positively charged and hydrophobic amino acid residues, respectively. The slash mark represents the cleavage site for thrombin.

recognition for fibrinogen. Additionally, the side chains of the amino acid monomers were necessary for the affinity of NPs to proteins.

3.3. Molecular docking study to determine the interaction between amino acid monomers and fibrinogen

Molecular docking was employed to virtually predict the binding forces of NPs to fibrinogen based on various scoring functions. We chose the amino acid monomers of NPs as ligands and the fibrinogen D domain as the receptor in the molecular docking study (Table 2 and Fig. 3), because the negatively charged D domain is the binding site for the positively charged E_A and E_B.

From Table 2, we observed that the docking Grid score of the five monomers and fibrinogen was the sum of the individual van der Waals force (Grid_vdw) and the electrostatic force (Grid_es). The docking Grid score of AArg was the highest (−54.16 kcal/mol), in which the contribution from the van der Waals force (Grid_vdw=−26.72 kcal/mol) was similar to that from electrostatic force (Grid_es=−27.43 kcal/mol). Furthermore, the docking Grid score of ALys took the second place (Grid score=−50.84 kcal/mol), and its Grid_vdw score and Grid_es score were −20.75 kcal/mol and −30.08 kcal/mol, respectively, similar to that of AArg. The Grid score of the other three monomers, APhe, ALeu, and AGlu, was −30.98, −32.80, and −35.38 kcal/mol, respectively. This was much lower than that of AArg and ALys because these three monomers all had much weaker electrostatic forces to fibrinogen D domain, and their Grid_es scores were −9.30 kcal/mol (APhe), −10.65 kcal/mol (ALeu), and −17.69 kcal/mol (AGlu), respectively. These results suggested that the two positively charged monomers (AArg and ALys) could strongly interact with fibrinogen not only via van der Waals force but also using electrostatic interactions. In contrast, the amino acid monomers with hydrophobic side chains (APhe and ALeu) or negative charge (AGlu) could not form strong electrostatic interaction with fibrinogen. These results were consistent with the binding assay. Based on the results of the binding assay and the Grid score from the molecular docking study, we speculated that the negatively charged D domain might be the predominant binding site for the positively charged AArg@NPs and ALys@NPs to fibrinogen.

Table 2
Affinity binding results for the fibrinogen D domain interacting with the five amino acid monomers using a molecular docking study.

Monomers	Grid score[a] (kcal/mol)	Grid_vdw[b] (kcal/mol)	Grid_es[c] (kcal/mol)
APhe	−30.98	−21.68	−9.30
ALeu	−32.80	−22.15	−10.65
AGlu	−35.38	−17.69	−17.69
ALys	−50.84	−20.75	−30.08
AArg	−54.16	−26.72	−27.43

[a] The sum of the van der Waals force (Grid_vdw) and the electrostatic force (Grid_es).
[b] The docking Grid score due to van der Waals force.
[c] The docking Grid score due to electrostatic force.

The binding models of fibrinogen and the various amino acid monomers via hydrogen bonds and hydrophobic interactions are shown in Fig. 3. Here, the amide carbonyl (>*O*═C−NH-) of AArg, ALeu, APhe and AGlu (acting as the acceptor) formed hydrogen bonds with the guanidine group (NH_2^+=C(NH_2)−NH-) in the Arg275 residue of fibrinogen (acting as the donor). In the case of the ALys monomer, the hydrogen bond was formed between the amide carbonyl (>*O*═C−NH-) of ALys (acting as the acceptor) and the primary amine group (NH_3^+-) in the Lys321 residue (acting as the donor). Furthermore, the carbonyl group on the amino acids, ALys and AGlu, might form intramolecular hydrogen bonds with their own hydroxyl, which may lead to the weakening of the interaction of both ALys@NPs and AGlu@NPs and fibrinogen compared with AArg@NPs. Additionally, with regard to the hydrophobic interactions, the Lys321 residue of fibrinogen acted as the main anchor residue to form hydrophobic interactions with the carbon-carbon skeletal chain of the five amino acid monomers. From these results, we inferred that the amino acid side chains with different polarity, amphiphilicity, chain length, and conformational rigidity had a major influence on the affinity to fibrinogen. These resulted in the different Grid scores and different main anchor residues of fibrinogen for these five amino acid monomers (Fig. 3).

3.4. Specific binding of AArg@NPs to fibrinogen

The specificity of AArg@NPs to fibrinogen was investigated by incubating AArg@NPs with a mixture containing a solution of three human plasma proteins, fibrinogen, γ-globulin, and HSA. After centrifugation, the supernatant and the precipitate were separated, and then the proteins bound to AArg@NPs were eluted from the pellet at 4 °C. This is because AArg@NPs would be highly hydrated and dispersed to release the proteins below 16 °C, while they would be aggregated together to encapsulate and capture proteins above 16 °C. The supernatant of the centrifuged solution and the elution from precipitation were both analyzed (Fig. 4) by SDS-PAGE.

In the supernatant of the centrifuged solution (Lane 6; Fig. 4), the bands of γ-globulin and HSA could be seen clearly, while no fibrinogen band was observed. This suggested that the γ-globulin and HSA were not bound firmly to the AArg@NPs, and that they could be easily separated from the AArg@NPs-protein complex or free AArg@NPs by centrifugation. However, we found a distinct band corresponding to fibrinogen in Lane 7 (the elution from precipitation), which indicated that the AArg@NPs could specifically bind fibrinogen with a strong affinity from the mixture of three proteins. These findings demonstrated that a single synthetically optimized NP formulation (AArg@NPs) could be used to capture fibrinogen specifically and selectively from human plasma proteins and may be used as an affinity reagent for fibrinogen.

4. Conclusions

In this study, the acryloylated derivatives of natural amino acids were prepared and used as functional monomers to synthesize five

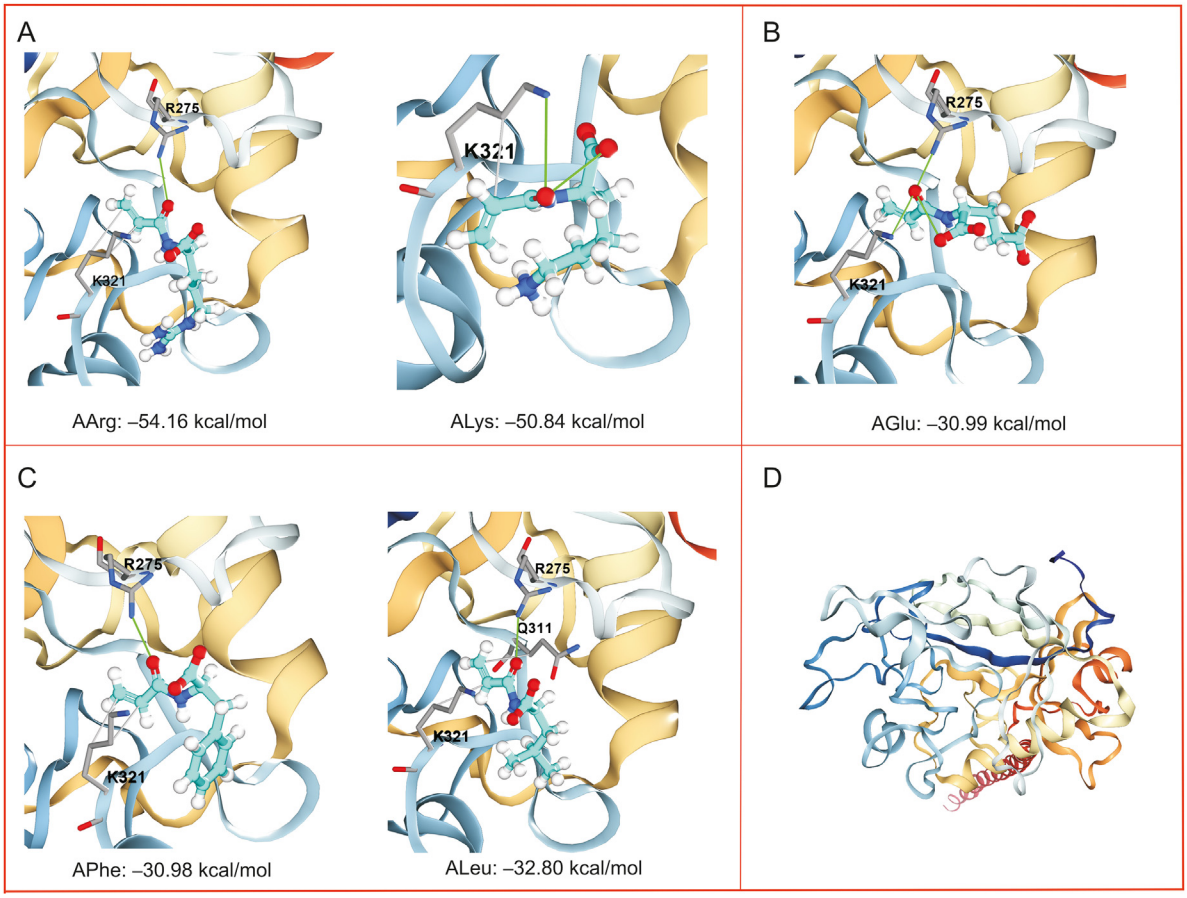

Fig. 3. Binding models of (A) positively charged AArg and ALys, (B) negatively charged AGlu, and (C) hydrophobic APhe and ALeu. Hydrogen bonds were depicted by solid green lines and hydrophobic interaction by solid gray lines. (D) The structure of the C chain of fibrinogen D domain.

amino acid polymer nanoparticles, including APhe@NPs, ALeu@NPs, AGlu@NPs, ALys@NPs, and AArg@NPs. These NPs were all stably dispersed in water at a nano-size scale. The incorporation of the temperature-sensitive monomer, NIPAm, allowed for the five NPs to show excellent temperature responsiveness, in which APhe@NPs, ALeu@NPs, and AGlu@NPs had specific LCSTs. In contrast, the other two NPs with positively charged side chains, ALys@NPs and AArg@NPs, would become aggregated above critical phase transition temperature (12 and 16 °C, respectively) but dispersed when lowering the temperature. After incubation with three human plasma proteins, the two positively charged NPs, ALys@NP and AArg@NPs, had a much more selective affinity for human fibrinogen compared with NPs with hydrophobic (APhe@NPs and ALeu@NPs) or negatively charged side chains (ALeu@NPs). This enhanced affinity is probably because ALys@NPs and AArg@NPs with hydrophobic and positively charged domains could strongly bind to the negatively charged and hydrophobic fragment D domain of human fibrinogen, which is consistent with the molecular docking results. Furthermore, AArg@NPs displayed excellent specificity for fibrinogen, since its binding amount to human fibrinogen was 2.3 times that of γ-globulin and 9 times that of HSA in the binding specificity assay. This allowed for the accurate identification and capture of human fibrinogen from a mixture of three human plasma proteins in the selective binding study. These results indicated that AArg@NPs was a strong candidate for use in the development of an affinity reagent for human fibrinogen. Additionally, AArg@NPs could easily switch between expansion and contraction in water using temperature changes. This probably allows AArg@NPs to possess the ability to catch and release the target protein fibrinogen from a complex biological sample in a reversible and temperature-responsive manner.

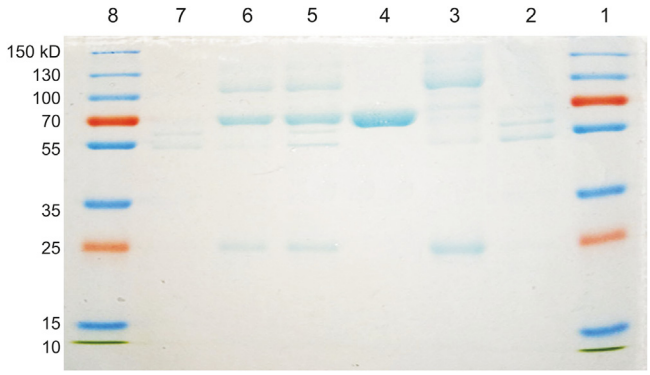

Fig. 4. Immunoprecipitation of fibrinogen with AArg@NPs by SDS-PAGE analysis. Lanes 1 and 8: molecular weight marker. Lane 2: fibrinogen. Lane 3: γ-globulin. Lane 4: HSA. Lane 5: protein mixture. Lane 6: supernatant of the centrifuged solution. Lane 7: the elution from precipitation. The SDS-PAGE gel was stained with Coomassie Brilliant Blue G-250.

Declaration of competing interest

The authors declare that there are no conflicts of interest.

Acknowledgments

This work was supported by the Natural Science Foundation of Guangdong Province, China (Grant No.: 2017A030313775), the Science and Technology Planning Project of Guangdong Province, China (Grant No.: 2016A010103016), and the Science and Technology Planning Project of Guangzhou City of Guangdong Province, China (Grant No.: 201607010148).

Appendix A. Supplementary data

Supplementary data to this article can be found online at https://doi.org/10.1016/j.jpha.2020.10.004.

References

[1] M. Bialkower, H. McLiesh, C.A. Manderson, et al., Rapid paper diagnostic for plasma fibrinogen concentration, Analyst 144 (2019) 4848–4857.
[2] S. Duga, R. Asselta, E. Santagostino, et al., Missense mutations in the human beta fibrinogen gene cause congenital afibrinogenemia by impairing fibrinogen secretion, Blood 95 (2000) 1336–1341.
[3] C. Velik-Salchner, T. Haas, P. Innerhofer, et al., The effect of fibrinogen concentrate on thrombocytopenia, J. Thromb. Haemostasis 5 (2007) 1019–1025.
[4] H.K. Stinger, P.C. Spinella, J.G. Perkins, et al., The ratio of fibrinogen to red cells transfused affects survival in casualties receiving massive transfusions at an army combat support hospital, J. Trauma: Inj. Infect. Crit. Care 64 (2008) S79–S85.
[5] B.M. Elliott, L.M. Aledort, Restoring hemostasis: fibrinogen concentrate versus cryoprecipitate, Expet Rev. Hematol. 6 (2013) 277–286.
[6] J.H. Levy, I. Welsby, L.T. Goodnough, Fibrinogen as a therapeutic target for bleeding: a review of critical levels and replacement therapy, Transfusion 54 (2014) 1389–1405.
[7] S.H. Lee, Y. Hoshino, A. Randall, et al., Engineered synthetic polymer nanoparticles as IgG affinity ligands, J. Am. Chem. Soc. 134 (2012) 15765–15772.
[8] A. Vijayan, P.P. James, C.K. Nanditha, et al., Multiple cargo deliveries of growth factors and antimicrobial peptide using biodegradable nanopolymer as a potential wound healing system, Int. J. Nanomed. 14 (2019) 2253–2263.
[9] K. Yoshimatsu, B.K. Lesel, Y. Yonamine, et al., Temperature-responsive "catch and release" of proteins by using multifunctional polymer-based nanoparticles, Angew. Chem. 124 (2012) 2455–2458.
[10] H. Koide, K. Yoshimatsu, Y. Hoshino, et al., A polymer nanoparticle with engineered affinity for a vascular endothelial growth factor ($VEGF_{165}$), Nat. Chem. 9 (2017) 715–722.
[11] K. Yoshimatsu, H. Koide, Y. Hoshino, et al., Preparation of abiotic polymer nanoparticles for sequestration and neutralization of a target peptide toxin, Nat. Protoc. 10 (2015) 595–604.
[12] J. O'Brien, S.H. Lee, S. Onogi, et al., Engineering the protein corona of a synthetic polymer nanoparticle for broad-spectrum sequestration and neutralization of venomous biomacromolecules, J. Am. Chem. Soc. 138 (2016) 16604–16607.
[13] X. Wang, H. Gan, M.X. Zhang, et al., Modulating cell behaviors on chiral polymer brush films with different hydrophobic side groups, Langmuir 28 (2012) 2791–2798.
[14] H. Skaat, R. Chen, I. Grinberg, et al., Engineered polymer nanoparticles containing hydrophobic dipeptide for inhibition of amyloid-β fibrillation, Biomacromolecules 13 (2012) 2662–2670.
[15] P. Dutta, J. Dey, Drug solubilization by amino acid based polymeric nanoparticles: characterization and biocompatibility studies, Int. J. Pharm. 421 (2011) 353–363.
[16] A.R. Kallar, J. Muthu, S. Selvam, Bioreducible amino acid-derived polymeric nanoparticles for delivery of functional proteins, Colloids Surf. B Biointerfaces 164 (2018) 396–405.
[17] J.V. González-Aramundiz, M.V. Lozano, A. Sousa-Herves, et al., Polypeptides and polyaminoacids in drug delivery, Expet Opin. Drug Deliv. 9 (2012) 183–201.
[18] H. Xu, Q. Yao, C. Cai, et al., Amphiphilic poly(amino acid) based micelles applied to drug delivery: the in vitro and in vivo challenges and the corresponding potential strategies, J. Contr. Release 199 (2015) 84–97.
[19] Y. Zhu, R. Liu, H. Huang, et al., Vinblastine-loaded nanoparticles with enhanced tumor-targeting efficiency and decreasing toxicity: developed by one-step molecular imprinting process, Mol. Pharm. 16 (2019) 2675–2689.
[20] B. Song, F. Wang, Y. Guo, et al., Protein-protein interaction network-based detection of functionally similar proteins within species, Proteins 80 (2012) 1736–1743.
[21] J. Rodríguez-Hernández, S. Lecommandoux, Reversible inside-out micellization of pH-responsive and water-soluble vesicles based on polypeptide diblock copolymers, J. Am. Chem. Soc. 127 (2005) 2026–2027.
[22] X. Wang, H. Gan, M. Zhang, et al., Modulating cell behaviors on chiral polymer brush films with different hydrophobic side groups, Langmuir 28 (2012) 2791–2798.
[23] A. Zengin, U. Tamer, T. Caykara, Extremely sensitive sandwich assay of kanamycin using surface-enhanced Raman scattering of 2-mercaptobenzothiazole- labeled gold@silver nanoparticles, Anal. Chim. Acta 817 (2014) 33–41.
[24] S. Bersani, S. Salmaso, F. Mastrotto, et al., Star-like oligo-arginyl-maltotriosyl derivatives as novel cell-penetrating enhancers for the intracellular delivery of colloidal therapeutic systems, Bioconjugate Chem. 23 (2012) 1415–1425.
[25] Y. Yonamine, K. Yoshimatsu, S.H. Lee, et al., Polymer nanoparticle-protein interface. Evaluation of the contribution of positively charged functional groups to protein affinity, ACS Appl. Mater. Interfaces 5 (2013) 374–379.
[26] P.T. Lang, S.R. Brozell, S. Mukherjee, et al., Dock 6: combining techniques to model RNA-small molecule complexes, RNA 15 (2009) 1219–1230.
[27] Y. Hoshino, T. Urakami, T. Kodama, et al., Design of synthetic polymer nanoparticles that capture and neutralize a toxic peptide, Small 5 (2009) 1562–1568.
[28] B. Chou, P. Mirau, T. Jiang, et al., Tuning hydrophobicity in abiotic affinity reagents: polymer hydrogel affinity reagents for molecules with lipid-like domains, Biomacromolecules 17 (2016) 1860–1868.
[29] J. O'Brien, K.J. Shea, Tuning the protein corona of hydrogel nanoparticles: the synthesis of abiotic protein and peptide affinity reagents, Acc. Chem. Res. 49 (2016) 1200–1210.
[30] M. Sponchioni, P.U. Capasso, D. Moscatelli, Thermo-responsive polymers: applications of smart materials in drug delivery and tissue engineering, Mater. Sci. Eng. C Mater. Biol. Appl. 102 (2019) 589–605.
[31] A. Bordat, N. Soliman, C.I. Ben, et al., The crucial role of macromolecular engineering, drug encapsulation and dilution on the thermoresponsiveness of UCST diblock copolymer nanoparticles used for hyperthermia, Eur. J. Pharm. Biopharm. 142 (2019) 281–290.
[32] E.N. Pederson, G. Interlandi, Oxidation-induced destabilization of the fibrinogen αC-domain dimer investigated by molecular dynamics simulations, Proteins 87 (2019) 826–836.